Chemical Engineering Journal 506 (2025) 160225

Contents lists available at ScienceDirect

Chemical Engineering Journal

journal homepage: www.elsevier.com/locate/cej

Impact of in–situ bioelectric field on biogas production, membrane fouling and microbial community in an anaerobic membrane bioreactor under sulfadiazine stress

Haojie Huang [a,b], Yutong Sun [a,b], Qing Du [a,b], Fu Gao [a,b], Zi Song [a,b], Zhiwen Wang [c], Suyun Chang [d], Xinbo Zhang [a,b,*], Wenshan Guo [e,a], Huu Hao Ngo [e,a,*]

[a] Joint Research Centre for Protective Infrastructure Technology and Environmental Green Bioprocess, School of Environmental and Municipal Engineering, Tianjin Chengjian University, Tianjin 300384, China
[b] Tianjin Key Laboratory of Aquatic Science and Technology, Tianjin Chengjian University, Jinjing Road 26, Tianjin 300384, China
[c] Frontier Science Center for Synthetic Biology and Key Laboratory of Systems Bioengineering (Ministry of Education), SynBio Research Platform, Collaborative Innovation Center of Chemical Science and Engineering (Tianjin), Department of Biochemical Engineering, School of Chemical Engineering and Technology, Tianjin University, Tianjin 300072, China
[d] Tianjin Hydraulic Research Institute, Tianjin 300000, China
[e] Centre for Technology in Water and Wastewater, School of Civil and Environmental Engineering, University of Technology Sydney, Sydney, NSW 2007, Australia

ARTICLE INFO

Keywords:
Anaerobic membrane bioreactor
Microbial fuel cell
Sulfadiazine
Membrane fouling
Microbial analysis

ABSTRACT

The treatment of swine wastewater (SW) using an anaerobic membrane bioreactor (AnMBR) shows significant potential for energy recovery. However, antibiotics in SW, such as sulfadiazine (SDZ), can inhibit microbial activity, leading to reduced operational efficiency and severe membrane fouling. This study investigated the performance of an integrated microbial fuel cell (MFC)-AnMBR system under various SDZ concentrations, focusing on methane production, membrane fouling, and microbial community dynamics. Results showed the bioelectric field in the MFC-AnMBR improved COD removal by 2.8%–7.3%, enhanced methane production by 12.5%–35.5%, and reduced volatile fatty acids (VFAs) accumulation by 35.3%–56.1% under SDZ stress, compared to a conventional AnMBR (C-AnMBR). Meanwhile, the bioelectric field reduced soluble microbial products (SMP) by 6.3%–43.0%, extracellular polymeric substances (EPS) by 21.9%-43.3% and extended the membrane fouling cycle by over 36 days than C-AnMBR under SDZ stress. Microbial analysis revealed that SDZ stress caused a 2.8%–7.8% reduction in methanogen populations within the MFC-AnMBR, 0.5%–3.0% higher than in the C-AnMBR due to the bioelectric field's influence. Moreover, the bioelectric field enriched *p_Chloroflexi*, which may help mitigate membrane fouling. In conclusion, the bioelectric field significantly enhances the overall performance of AnMBR systems under SDZ stress, improving energy recovery and membrane fouling resistance.

1. Introduction

Intensive swine farms meet the growing demand for swine protein products and generate large quantities of swine wastewater (SW). SW mainly consists of food residues, flushing and fecal wastewater from the farming process, characterized by high concentrations of organic matter, nitrogen, phosphorus, antibiotics, etc [1]. Discharge of these components poses significant risks, including water and soil contamination, environmental degradation and the dissemination of resistance genes, thereby amplifying environmental health risks [2]. With the expanding scale of intensive farming, effective SW treatment has become crucial.

To address this issue, numerous countries have enacted policies to support the treatment and recycling of livestock wastewater [3]. As a sustainable wastewater treatment technology, anaerobic digestion is gaining attention in treating SW [4,5]. Its main advantages include renewable energy production, low energy consumption and low sludge production. However, removing slow-growing anaerobic microorganisms remains a significant problem for effective anaerobic digestion.

Notably, the anaerobic membrane bioreactor (AnMBR) combines the advantages of both anaerobic technology and membrane filtration,

* Correspondence authors.
E-mail addresses: zxbcj2006@126.com (X. Zhang), ngohuuhao121@gmail.com (H.H. Ngo).

https://doi.org/10.1016/j.cej.2025.160225
Received 12 November 2024; Received in revised form 31 January 2025; Accepted 2 February 2025
Available online 3 February 2025

enhancing organic matter removal and energy recovery, making it well–suited for SW treatment [6]. Reports showed that AnMBR could achieve chemical oxygen demand (COD) removal exceeding 95.0%, significantly higher than conventional anaerobic systems (~ 80.0%) in SW treatment [7,8]. However, the widespread application of AnMBR technology in SW still needs to be improved by problems such as high concentrations of nitrogen, phosphorus and antibiotics, with antibiotic stress being a critical bottleneck [9]. Antibiotic stress not only inhibits microbial activity and causes a decrease in methanogenesis but also increases membrane pollutants (soluble microbial products (SMP) and extracellular polymeric substances (EPS)), thus exacerbating membrane fouling [10]. For example, Zhang et al. observed a decrease in biogas production of approximately 16.3% and a reduction in membrane fouling cycle from 23 days to 12 days with the addition of 0.5 mg/L antibiotics; this reduction further decreased to about 36.1% and 7 days, respectively, when the antibiotic concentration increased to 1.0 mg/L in AnMBR [11]. Severe membrane fouling and the consequent frequent cleaning requirements have substantially increased the operational costs of AnMBRs, significantly restricting their extensive use in the treatment of antibiotic-containing swine wastewater [9]. Therefore, ensuring efficient SW treatment by AnMBR while mitigating antibiotic stress is crucial to promote the application of AnMBR in SW treatment and resource recovery [12].

In recent years, the integration of microbial fuel cells (MFCs) with AnMBRs has emerged as an integrated system to alleviate membrane fouling, improve effluent quality, and increase energy production [12–17]. The integrated MFC-AnMBR system enhances bioactivity by facilitating electron transfer between ectroactive and anaerobic bacteria [15]. The self-generated bioelectric field within the integrated system effectively prevented the deposition of negatively charged pollutants on the membrane module through electrostatic repulsion, which greatly alleviates membrane fouling. For example, Hou et al. found that the concentration of SMP & EPS dramatically declined, and the operational time was prolonged for 16 days in the MFC-MBR integrated system, suggesting that the spontaneous micro-electric field could alleviate the membrane fouling [18]. Similar conclusions were obtained by Huang et al.; the MFC-MBR integrated system extended the membrane fouling cycle by at least 40 days and achieved a methane gain of 54.2% [15]. Nevertheless, extant research overlooked the impacts of antibiotics present in swine wastewater on the operation of the MFC-AnMBR system. Currently, the mechanism of the integrated MFC-AnMBR system relieving the inhibitory effects triggered by antibiotic stress during SW treatment remains obscure. Consequently, a comprehensive and systematic analysis of this aspect is urgently required.

This study is therefore to investigate the operation performance of the integrated MFC-AnMBR system in the presence of broad-spectrum antibiotic SDZ in SW. The main objectives are: (1) to analyze the enhancement performance of the MFC-AnMBR integrated system under SDZ stress based on the investigation of the effects of SDZ on the removal of organic matter and methane generation in the AnMBR system, (2) to explore the membrane fouling allevation by bioelectric field in the MFC-AnMBR integrated system, (3) to investigate the microbial community enrichment and methanogenic activity in the presence of SDZ and bioelectric field, respectively, and (4) to comprehensively elucidate the regulation mechanism of bioelectric field in enhancing the SW treatment in the integrated AnMBR system. This work can help deeply understand the influence of the in–situ bioelectric field on enhancing the operation stability and performance of an anaerobic membrane bioreactor under antibiotic stress, thereby guiding the application of the integrated AnMBR system in treating natural wastewater.

2. Materials and methods

2.1. Operation of the systems

Fig. 1 shows the two sets of devices used. The MFC-AnMBR system is named R1, while the conventional AnMBR is denoted as R2. Both reactors were composed of plexiglass, featuring an inner diameter of 13.0 cm, a height of 31.5 cm, and an effective operational volume of 2.0 L. The temperature within the reactors was rigorously maintained at 35°C through a circulating thermostatic water bath (Bilang Experimental Instrument Manufacturing Co. Ltd, Wuxi, China).

The filter membrane module in the reactors was made of polyvinylidene fluoride (PVDF) hollow fiber membrane (Haike Membrane Technology Co. Ltd, Guangzhou, China) with a pore size of 0.1 μm and a specific surface area of 0.042 m^2. The reactors' water influent and effluent flow rates were adjusted via the pump speed. Transmembrane pressure (TMP) was monitored by a pressure sensor (MBS1900, Danfoss, Denmark) alongside a paperless recorder (BRW500–5100, Fü rest). Biogas produced was systematically collected utilizing aluminum foil biogas collection bags. Furthermore, a fraction of the generated biogas was recirculated back into the reactor for stirring using a vacuum pump (D50 remote control type, Chengdu Hailin Technology Co., Ltd, China) at the aeration frequency of 1 min/40 min.

The MFC-AnMBR system was distinctively structured to encompass an AnMBR and a single–chamber air–cathode MFC configuration. The AnMBR functioned as the MFC anode chamber, housing both an anode electrode and the membrane module.

Both systems were operated continuously during the experimental phase for 90 days each. Under the same influent conditions, both systems were constantly operated with a hydraulic retention time of 96 h. According to the previous study [11], the experiments were divided into

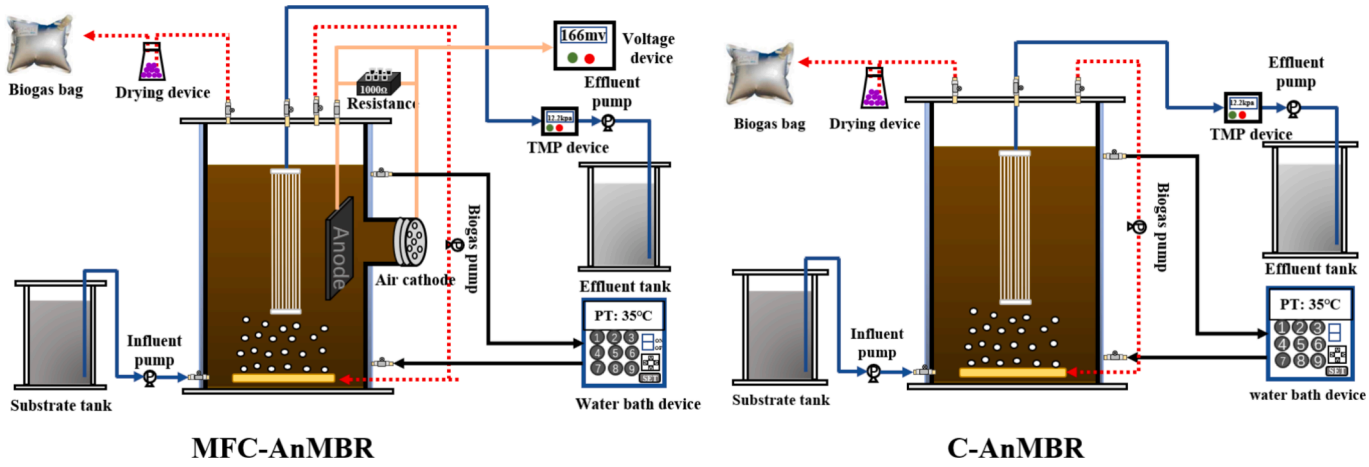

Fig. 1. The diagram of the two sets of devices.

phase S1, phase S2 and phase S3 according to the influent SDZ concentration, corresponding to SDZ concentrations of 0, 0.5 and 1.0 mg/L, respectively.

2.2. Materials and chemicals

The anaerobic sludge used in the experiment was taken from the anaerobic digester in a wastewater treatment plant (Tianjin, China). The mixed liquid suspensions (MLSS) and mixed liquid volatile suspensions (MLVSS) in R1 and R2 were appropriately 11.1 g/L and 7.3 g/L, respectively.

The wastewater used in this experiment was synthetic swine wastewater consisting of glucose as the primary carbon source. Different SDZ concentrations were added in various phases of the experiment. The main components of synthetic swine wastewater were $C_6H_{12}O_6$ (9000 mg/L), NH_4Cl (360 mg/L), KH_2PO_4 (360 mg/L), $FeCl_2$ (112 mg/L), $MgSO_4$ (30 mg/L) and small amounts of essential trace elements. The essential trace elements included $MnCl_2$ (1 mg/L), $ZnCl_2$ (1 mg/L), $NiCl_2$ (21 mg/L), $CoCl_2$ (13 mg/L), $CuCl_2$ (0.25 mg/L), H_3BO_3 (0.05 mg/L), and Na_2MoO_4 (0.24 mg/L). The stock solutions of SDZ were prepared by dissolving 10 mg of antibiotics in 100 mL of sodium hydroxide solution and stored in brown bottles at –4℃.

2.3. Analysis methods

COD was measured following the standard method (APHA, 2012). The pH was detected using a portable pH meter (HACH HQ11D, USA). Biogas components were analyzed by gas chromatography (GC–2014, Shimadzu, Japan). The parameters were inlet temperature of 150℃, column temperature of 50°C, and balance time of 3 min. The detector temperature was 180°C, the data acquisition sampling rate was 40 msec, the end time was 5 min, the current was 35 mA, and the pretreatment temperature was 200°C. Volatile fatty acids (VFAs) were detected by gas chromatography (PerkinElmer Clarus, USA). The equipment's set parameters are as follows: the automatic injection volume is 20 μL, the mobile phase is 0.05% dilute phosphoric acid, and the flow rate is 0.7 mL/min. The analysis Column model is CosmosilPacked column 5C18-PAQ (5 μm, 4.6 × 250 mm), and the column temperature chamber is set at 45℃. The detector is an ultraviolet detector, and the wavelength measured by the detector is 210 nm. MLSS and MLVSS were determined by the gravimetric method [19]. The SMP was extracted by centrifugal filtration, and the mixture of EPS and sludge was further separated by pyrolysis. Polysaccharides and proteins in SMP and EPS were analyzed using phenol–sulfuric acid and Forint–Ciocalteu methods [20]. Sludge particle size and sludge surface charge were determined using a Malvern laser particle size analyzer (Malvern Masters Sizer 2000, Malvern Instruments, UK) and a zeta potential analyzer. The concentration of SDZ was tested by high-performance liquid chromatography-triple quadrupole mass spectrometry (LC-MS8050, Shimadzu, Japan). Solid phase extraction (SPE) was used as pre-treatment for SDZ analysis, and the extraction cartridge was Oasis (HLB) (500 mg, 6 cc, Waters, USA). The column type was Shimadzu-packGISTC18 (size 2.1 mm, length 2 μm), and the column temperature was set at 40 °C. The interface temperature was set at 300℃, the interface voltage was 4 kV, and the interface current was 1.7 μA. The flow rate of the mass spectrometer dryer was 10 L/min, and the temperature of the heating block was set at 400 °C. The mobile phase components were 0.1% formic acid solution and acetonitrile solution in a volume ratio of 20:80, the flow rate of the mobile phase was 0.4 mL/min, the autosampling volume was set to 5 μL, and the program run time was set to 3 min. The linear calibration curve is $y = 2.50760{\cdot}107x + 16502$, the correlation coefficients R2 were > 0.9990, the recovery was 77.12%-126.37%, the detection limit was 0.001–0.260 ng/L, and the relative standard deviation was $< 9.34\%$.

2.4. Microbial community analysis

The dynamics of microbial community structure were examined by NGS analysis. At the end of each phase, sludge samples on the membrane were analyzed using 16S rRNA sequencing to evaluate the changes in the microbial community.

DNA was extracted using the E.Z. N.A.® soil kit (Omega Bio TEK, Norcross, GA, USA). The concentration and purity of DNA were detected by Nanodrop 2000, and the quality of DNA extraction was confirmed by 1.0% agarose gel electrophoresis. PCR amplification of the variable region of colony V3–V 4 was conducted with primers 515F (GTGCCAGCMGCCGCGG) and 806R (GGACTACHVGGGTWTCTAAT). The PCR products were detected and quantified using QuantiFluor™–ST (Promega, USA) and then sequenced on Illumina's Miseq PE300 platform from Illumina (commissioned by Shanghai Meiji Biomedical Technology Co., Ltd.). Raw sequences were quality–controlled using the Trimmomatic software, spliced using the FLASH software and clustered using the UPARSE software (version 7.1 https://drive5.com/uparse/) based on 97.0% similarity to OTU. In the meantime, single sequences and chimeras were removed during clustering. Each line was annotated with species classification using the RDP classifier (https://rdp.cme.msu.edu/), compared to the Silva database (SSU123), and a comparison threshold of 70.0% was established.

2.5. Genetic analysis

To further investigate SDZ's effect on VFAs and methane production, the metabolic pathways involved in these processes were analyzed, as well as the expression of related functional genes, based on the annotation analysis of the KEGG database.

Appropriate quantities of suspended sludge were retained at the end of each phase for metagenomics sequencing. DNA extraction was performed using the E.Z. N.A.® Soil DNA Kit (Omega Bio–tek, USA). After DNA extraction, DNA concentration and purity were checked, and DNA integrity was examined by 1 % agarose gel electrophoresis. The DNA was fragmented by Covaris M220 (Genetics, China), fragments of about 400 bp were screened, and libraries were constructed using NEXTFLEX Rapid DNA–Seq (Bioo Scientific, USA). Macro–genome sequencing was performed using the Illumina NovaSeq (Illumina, USA) sequencing platform (Shanghai Meiji Biomedical Technology Co., Ltd.). The original sequences were quality controlled using the software Fast and BWA; the optimized sequences were spliced and assembled using the software MEGAHIT; the ORFs of the contigs in the splicing results were predicted using the software Prodigal/MetaGene for ORFs prediction of contigs from splicing results; software CD–HIT for clustering and constructing non–redundant gene sets for gene sequences predicted from all the samples; and software SOAPaligner for counting the abundance information of genes. The amino acid sequences of the non–redundant gene sets were compared with the NR, KEGG and CARD databases using Diamond (BLASTP comparison parameter was set to a desired e–value of 1e–5), and the corresponding taxonomic, KEGG functional and antibiotic resistance functional annotations were obtained.

2.6. Data analysis

SPSS (version 22.0) was used for statistical analysis. Additionally, one-way analysis of variance (ANOVA) was used, with $p < 0.05$ considered statistically significant. The linear discriminant analysis (LDA) effect size algorithm (LEfSe) was applied to explore the statistically substantial features of microbial communities between different samples. The genetic statistical tests, such as the *t*-test, Wilcoxon signed rank test, and Pearson correlation test (where specified), were performed using R (version 3.5.3). Statistically significant was considered with the $P < 0.05$ [21]. The data of averages, standard deviations, and fold changes of ARGs were organized in Excel 2010 (Microsoft, USA). ARGs were considered statistically significantly enriched or depleted if

the mean fold change range of three standard deviations was entirely > 1.0 or < 1.0, respectively [22].

3. Results and discussion

3.1. Operational performance

3.1.1. Pollutants removal

As shown in Fig. 2a, in phase S1, both R1 and R2 showed stable and efficient COD removal of 99.3% ± 0.1% and 97.4% ± 0.3%, respectively. Significantly, R1 exhibited higher and more stable COD removal than R2. This phenomenon concurred with the research conducted by Huang et al., in which it was ascertained that the self-generated electric field of an MFC augmented COD removal by 8.75 ± 1.5% [11]. Thus, it can be inferred that the bioelectric field exerted a positive influence on enhancing the removal of organic substances, as corroborated by extant literature [11,23]. In phase S2, a sudden drop in COD removal to 90.3% in R2, followed by stabilization at 94.6% ± 1.4%, was observed. This decline was attributed to antibiotic shocks. Previous studies have shown that SDZ is a broad–spectrum antimicrobial agent that inhibits microbial activity, thereby reducing microbial degradation of pollutants [24]. In addition, the accumulation of difficult-to-degrade and toxic intermediates such as aniline and 2-aminopyrimidine during the degradation of SDZ can also decrease COD removal [25–27]. The subsequent rebound in COD removal was linked to microbial acclimatization [28]. During this period, R1 showed less than 1% reduction in COD removal, indicating that the bioelectric field could eliminate the toxicity of low amounts of SMs to microorganisms. Xu et al. have shown that MFCs can expedite the rate of electron transfer in redox reactions, and the electrical stimulation generated by MFCs can enhance microbial activity, thus promoting the removal of antibiotics [29]. These findings present substantial potential for applying this technology in treating antibiotic-containing wastewater [29,30].

Moving into phase S3, both R1 and R2 exhibited a decrease in COD removal, with the flowing COD concentration increasing from 64.6 mg/L to 496.3 mg/L in R1 and from 253.2 mg/L to 962.9 mg/L in R2. This result was consistent with Cheng et al.'s previous report [30]. As the total antibiotic concentration increased from 0 to 0.9 mg/L, the COD removal decreased from 94.2% to 18.8%, reflecting that the higher antibiotic concentration caused a more substantial inhibitory effect on the anaerobic microorganisms. Notably, R1 relied on the reinforcing effect of the bioelectric field to show only minor changes.

3.1.2. pH and VFAs

The pH is a macroscopic representation of VFAs, while VFAs directly affect the activity of methanogens and subsequently affect the anaerobic digestion process in the reactor. As shown in Fig. 2b, pH for R1 and R2 in phase S1 were 7.02 ± 0.02 and 6.82 ± 0.09, respectively, with corresponding VFAs concentrations of 480.6 mg/L and 996.2 mg/L. The VFAs concentration in R1 was 52.3% lower than in R2, correlating with a higher pH. This indicated that more VFAs were successfully utilized due to the bioelectric field stimulation, as evidenced by the higher methane production. This observation demonstrated that introducing an electrode block promotes efficient VFAs degradation, thereby reducing VFAs accumulation [31].

In phase S2, VFAs concentration increased by 22.8% in R1 and 28.2% in R2, decreasing pH to 6.96 ± 0.02 and 6.75 ± 0.13, respectively. Notably, R2 showed higher VFAs concentration and decreasing pH during the first 10 days of antibiotic dosing, likely due to the transient toxic effects of antibiotics [24]. Based on previous studies, SDZ

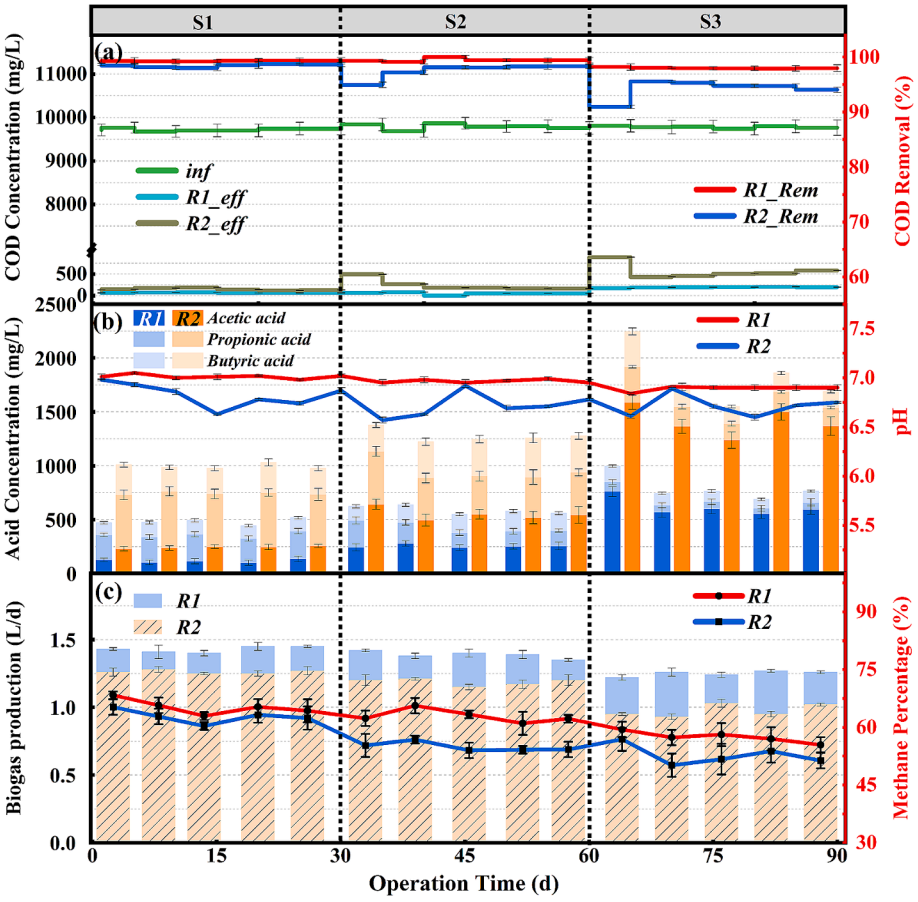

Fig. 2. Variation of (a) COD removal, (b) pH and VFAs, (c) Methane production.

prevented the addition of p-aminobenzoic acid to the folate molecule by competing for dihydropteroate synthase. Thus, SDZ inhibited the synthesis of folate required for the synthesis of purines and nucleic acids and thus limited bacterial growth [11,32]. Then, VFAs and pH gradually recovered as microorganisms adapted [28]. In contrast, R1 displayed good stability in VFAs and pH. This was attributed to the bioelectric field's ability to facilitate direct electron transfer between methanogens and electrobacteria [11]. Thus, the metabolic efficiency of methanogens was greatly improved, and the risk of system acidification was successfully avoided.

In phase S3, both R1 and R2 exhibited significant VFAs accumulation, with increases of 34.2% in R1 and 42.1% in R2, leading to notable pH decreases (6.89 ± 0.03 in R1 and 6.67 ± 0.13 in R2). This was in line with the report of Aydin et al., which reported that the concentration of VFA increased in a linear fashion, with the antibiotic concentration increasing from 0 to 250.0 mg/L [33].The higher SDZ concentration exacerbated the inhibition of anaerobic digestion, particularly affecting methanogens and causing VFAs accumulation [11]. In addition, it was noteworthy that the increase in VFAs concentration in both R1 and R2 during phases S2–S3 were primarily due to acetate accumulation, driven by antibiotic–stimulated enrichment of acetate–producing enzymes and inhibition of methanogenic enzymes (*detailed in sections 3.4*).

3.1.3. Methanogenic performance

As shown in Fig. 2c, the biogas production and methane percentage in R1 and R2 were monitored to evaluate the methanogenic performance. In phase S1, the biogas production in R1 and R2 was 1.43 ± 0.02 L/d and 1.24 ± 0.03 L/d, respectively, with methane percentage was 62.1% ± 2.1% and 60.8% ± 1.9%, respectively. Notably, the bioelectric field increased the biogas production and methane percentage by about 15.0% and 1.3%, respectively. This significant improvement can be attributed to the enrichment of electroactive bacteria in the MFC-AnMBR system, as explained by Huang et al. [11]. As these electroactive bacteria multiplied, they produced many free electrons, which enhanced the direct electron transfer from the methanogenic bacteria and thus facilitated the methanogenic process. In addition, microbial and genetic analysis in this study showed the bioelectric field increased the abundance of methanogens and related enzyme genes, thereby enhancing methane production (*detailed in sections 3.4*).

In phases S2 and S3, the biogas production and methane percentage in R1 and R2 exhibited varying decreases. Specifically, the biogas and methane percentage in R1 dropped to 1.39 ± 0.01 L/d and 59.3% ± 2.5%, and then to 1.17 ± 0.03 L/d and 54.1% ± 2.5%, and in R2, decreased from 1.13 ± 0.03 L/d and 55.0% ± 1.0% to 0.98 ± 0.04 L/d and 51.6% ± 1.6%, respectively. All these showed that the inhibition of anaerobic digestion was more severe with increasing SDZ concentration, resulting in lower biogas production, as evidenced by variations in VFAs. Previous studies have revealed that antibiotic use elevated lactate dehydrogenase, a cytoplasmic component originating from damaged cells and that its release signals compromised cellular integrity [34]. This finding further implied that the presence of SDZ effectively inhibited the growth of anaerobic bacteria and induced the process of anaerobic cell lysis. This process not only interfered with the proper conduct of anaerobic digestion but ultimately reduced methane production significantly. In addition, the gradual decrease in the abundance of methanogenic bacteria and their associated enzymes observed in this study strongly supports the above findings(see Section 3.4 for details). It was noteworthy that during this process, R1 showed higher and more stable methanogenic performance with higher methanogen abundance and associated enzyme abundance compared to R2, suggesting that the bioelectric field enhanced the resistance of methanogens to antibiotic-induced stress.

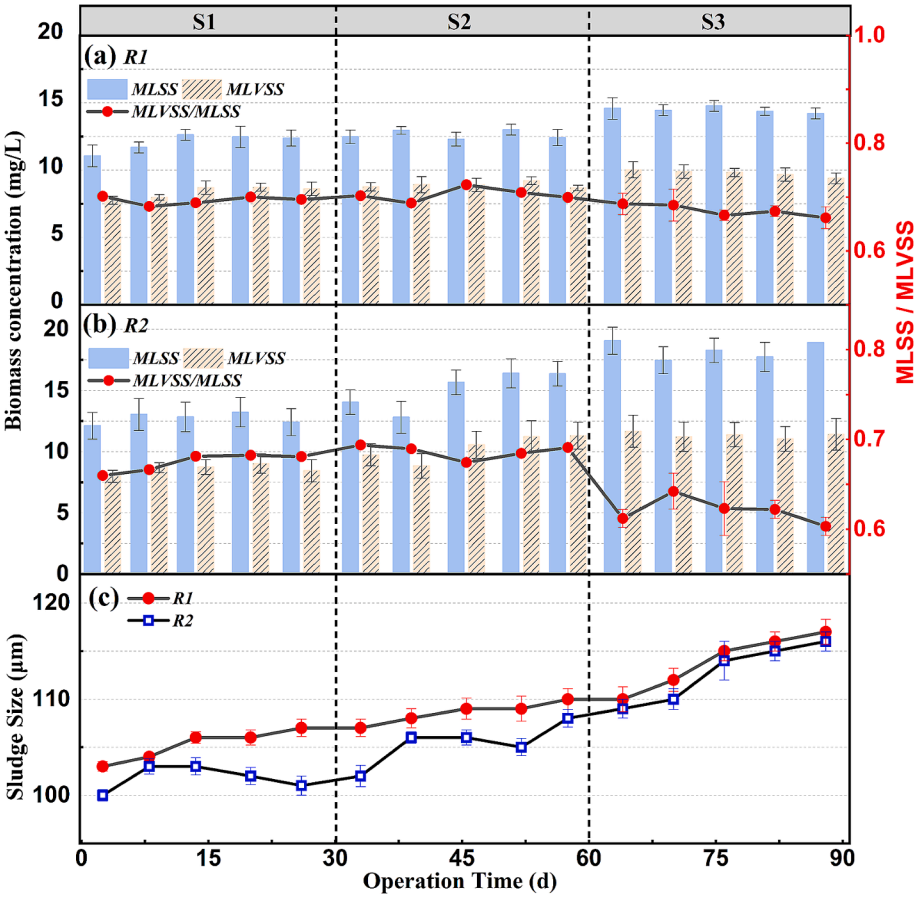

Fig. 3. Variation of (a) biomass in R1, (b) biomass in R2 and (c) sludge size.

3.1.4. Sludge characteristics

The fluctuations in MLSS and MLVSS were shown in Fig. 3. In phase S1, the MLSS and MLVSS concentrations were stabilized at 12.0 ± 0.6 g/L and 8.4 ± 0.4 g/L in R1, and 12.7 ± 0.4 g/L and 8.6 ± 0.4 g/L in R2, respectively. Notably, R1 exhibited a lower sludge yield compared to R2. The suspended solids tend to flocculate and accumulate in the sludge without anaerobic utilization, implying that undigested, digestible COD eventually converts to residual sludge [35]. The bioelectric field fostered COD to methane conversion and concurrently reduced COD conversion to sludge. This outcome is practical in lessening the burden associated with sludge treatment [31].

In phase S2, the concentrations of MLSS and MLVSS in R1 were similar to those in phase S1, while in R2, the concentrations increased by 18.3% and 20.4%, respectively. This showed that antibiotic exposure resulted in lower COD removal and promoted increased biomass in R2 [28]. In phase S3, both R1 and R2 showed a significant increase in biomass, with MLSS (MLVSS) rising by 14.6% (9.8%) in R1 and 21.5% (9.8%) in R2. All these showed that the inhibitory effect on anaerobic digestion would be more severe when the SDZ concentration was increased. However, the bioelectric field alleviated the negative impact caused by SDZ to some extent. Moreover, a marked decrease in the MLVSS/MLSS ratio was evident in phase S3, as the ratios for R1 and R2 dropped to 0.7 and 0.6, representing reductions of 4.2% and 9.6%, respectively. The MLVSS/MLSS ratio is an indicator for assessing activity within the system. Typically, effective activated sludge exhibits MLVSS/MLSS ratios in the range of 0.7 to 0.8, indicative of a substantial microbial presence and efficient pollutant removal [36]. R1 and R2 recorded MLVSS/MLSS ratios below 0.7 in phase S3, signaling the apparent inhibition of sludge activity. This inhibition was associated with how sulfonamide antibiotics could impede bacterial growth and reproduction. Sulfonamides mimic p–aminobenzoic acid (PABA), a precursor for folate biosynthesis, competing with PABA for dihydropteroate synthase bacteria utilize to synthesize folic acid. Thus, sulfonamides reduce the necessary folic acid levels for bacterial growth, hindering their replication [37]. Notably, compared to R2, R1 exhibited significantly less inhibited sludge activity, potentially due to the bioelectric field's ability to enhance the removal of sulfonamide, thus reducing the inhibitory effects [38].

As shown in Fig. 3c, both R1 and R2 exhibited an increasing trend in sludge particle size over the experimental phase, suggesting that antibiotic exposure did not influence this aspect significantly. However, compared to the fluctuating changes in R2, the sludge particle size in R1 steadily increased, reflecting a more stable anaerobic system in R1. Moreover, it was noteworthy that the sludge particle size in R1 was slightly more prominent than in R2, which could be a reason for potentially mitigating membrane fouling issues in R1.

3.2. Membrane fouling and mitigation mechanism

3.2.1. TMP

As shown in Fig. 4a, R2 experienced two severe membrane fouling (TMP > 35 kPa) during the experiment, with membrane fouling cycles of 69 and 35 days, respectively. In contrast, R1 remained in a slow fouling stage (TMP < 1 kPa) throughout the experiment, indicating the membrane fouling cycle in R1 was extended by at least 36 days. In AnMBR, the accumulation of membrane-fouling pollutants (solutes, colloids, microbial cells, etc.) smaller than the pore size leads to pore clogging and forming a cake layer. The cake layer formed due to the precipitation of microorganisms, EPS/SMP/biomass attachment, flocculent deposition, etc., onto the membrane surface [39]. This difference was

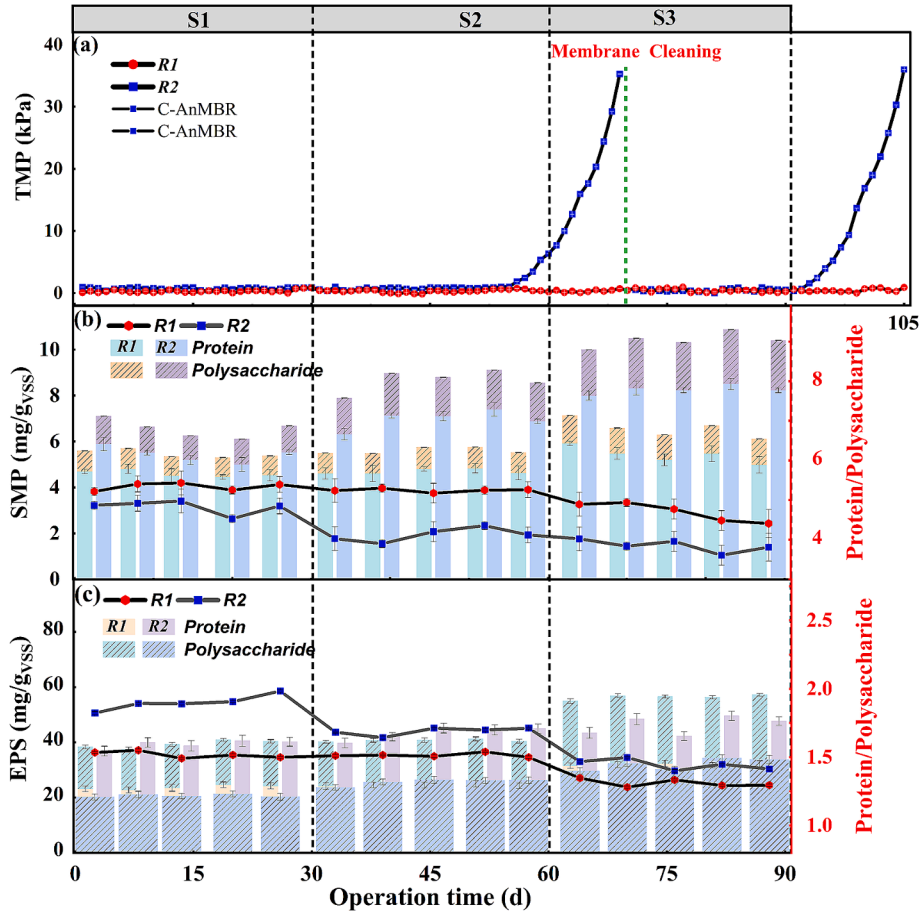

Fig. 4. Variation of (a) TMP (90–105 days for further observation), (b) SMP Concentration and (c) EPS Concentration.

primarily related to the larger sludge particle size in R1 (as described above) and the lower concentrations of membrane fouling contaminants and microbial community structure in R1 (see Sections 3.2.2 and 3.3.2 for details). Notably, the second membrane fouling cycle for R2 was nearly halved (69 and 35 days, respectively). This discrepancy was attributed to the increasing membrane pollutants (e. g., proteins and polysaccharides, as shown below) due to antibiotic exposure and the challenges associated with membrane cleaning. Higher concentrations of proteins and polysaccharides accelerated adhesion to the membrane, leading to membrane fouling [40]; membrane cleaning alone was insufficient to remove adherent fouling in membrane pores, resulting in faster membrane fouling formation [41]. All these demonstrated the membrane fouling challenges faced by AnMBR in treating antibiotic wastewater, which was significantly mitigated by the presence of the bioelectric field.

From the surface morphology of the membrane before and after fouling (Fig. S1), it can be seen that at the end of phase S1 on day 30, neither R1 nor R2 showed severe membrane fouling (TMP < 1 kPa). The membrane pores were still apparent at this phase, and there was no accumulation of filter cake layer on the surface. However, significantly fewer pollutants were adhering to the membrane pores in R1. This difference may be related to the lower concentration of SMP with a high protein/polysaccharide (PN/PS) ratio and larger particle size in R1. At day 105, R1 still did not show severe membrane fouling (TMP < 1 kPa), while the TMP in R2 had exceeded 35 kPa. From the SEM images, the R1′s membrane pores were still evident, but some reticulated pollutants similar to the pre–structure of the cake layer were observed on the membrane surface. On the other hand, a dense cake layer appeared on the R2′s membrane surface, and the distribution of the cake layer was very uneven and compact.

3.2.2. SMP and EPS

SMP and EPS are microbial metabolites with protein and polysaccharide–based compositions, which significantly affect membrane fouling [41]. As shown in Fig. 4b, in phase S1, the SMP concentrations in R1 and R2 were about 5.5 mg/gVSS and 6.5 mg/gVSS, with the PN/PS ratio of around 5.3 and 4.8, respectively. It was found that irreversible fouling resistance was proportional to higher SMP concentrations and a lower ratio of PN/PS in SMP [42]. Lower SMP concentration and higher PN/PS ratio in R1 suggested that the bioelectric field reduced the SMP concentrations (especially polysaccharides) and thus mitigated membrane fouling. The lower concentration of SMP in R1 was attributed to two reasons: firstly, the negatively charged SMP was adsorbed by the positively charged carbon felt electrode to form macromolecular precipitates [43], and secondly, the bioelectric field facilitated SMP degradation [18]. In phase S2, there was no significant change in SMP concentration and PN/PS ratio in R1, while SMP concentration in R2 increased to 8.7 mg/VG, and PN/PS ratio decreased to 4.1. This showed that the exposure to low antibiotics resulted in more cell lysis and thus increased SMP concentrations (especially proteins) for R2 [44]. Compared to R2, the SMP concentration and PN/PS ratio in R1 showed high stability, suggesting that the bioelectric field enhanced the shock resistance of the anaerobic system to the low SDZ concentration. In phase S3, both R1 and R2 showed an increase in SMP concentration to 6.6 mg/gVSS and 10.4 mg/gVSS, respectively, and a decrease in PN/PS ratio to 4.7 and 3.9, respectively. This showed that the exposure to higher concentrations of SDZ increased the harmful effects on microorganisms, which in turn secreted more SMP. Although R1 could metabolise in a low antibiotic environment, it was still not wholly resistant to the harmful effects of a high antibiotic environment. However, compared to R2, the bioelectric field in R1 reduced the SMP accumulation by about 37.0% and increased the PN/PS ratio by 22.1%, implying less irreversible fouling.

Similar to the SMP variations, the EPS concentration and PN/PS ratio in R1 remained in a stable range of around 40.0 mg/gVSS and 1.5 in phases S1 and S2, respectively, and changed to 56.4 mg/gVSS and 1.3 in phase S3. The EPS concentration in R2 gradually raised from 60.0 mg/gVSS to 68.9 mg/gVSS and 78.3 mg/gVSS, and the PN/PS ratio gradually dropped from 1.9 to 1.7 and 1.5, respectively, after exposure to SDZ. EPS production is an automatic response of microorganisms to toxic environments and is essential in protecting microorganisms from antibiotics. Microorganisms secrete more EPS to form a protective “cocoon” that delays the entry of harmful compounds into the cell body [45]. EPS change in R2 responded obviously to SDZ concentration variation. In contrast, it varied slightly in R1 at a high concentration of SDZ (phase S3), which further demonstrated that the bioelectric field increased the resistance of AnMBR to antibiotic exposure.

The PN/PS ratio variation was also remarkable, with a gradual decrease in the PN/PS ratio for R2 throughout the experiment and a drop in R1 only in phase S3. The microorganisms preferentially metabolized the polysaccharides in EPS. Thus, the decrease in the protein/polysaccharide ratio may be due to the gradual inhibition of SDZ to the microbial activity, increasing residual polysaccharides [31]. Furthermore, it was noteworthy that the PN/PS ratio was consistently lower in R1 than in R2 throughout the experiment. PN usually carries a positive charge from hydrolysis of the amino group. In contrast, PS had a negative charge from hydroxyl hydrolysis, and a lower PN/PS ratio in R1 implied a lower zeta potential [46]. Membrane modules usually accumulate large amounts of negatively charged SMPs and EPSs, resulting in electronegativity on the surface. As a result, the lower zeta potential of the EPSs in R1 was more likely to move away from the membrane surface through electrostatic repulsion in the presence of the bioelectric field. This also can be attributed to membrane fouling mitigation.

The 3D fluorescence spectra of SMPs and EPSs are shown in Fig. S2. Zone I is protein–like (tryptophan, tyrosine, etc.), Zone II is fulvic acid matter (FA), Zone III is humic acid matter (HA), and Zone IV is dissolved organic matter (DOM). In phase S1, the fluorescence intensity of DOM and HA in SMP and EPS was significantly lower in R1 than in R2, indicating accelerated degradation of these substances under the condition of bioelectric field. Furthermore, the high molecular weight (HMW) organic substances of FA, DOM, and HA were identified as primary contributors to membrane pore fouling [47,48]; therefore, the lower fluorescence intensity of HA and DOM in R1 also proved that the bioelectric field alleviated membrane fouling. In phases, S2 and S3, a more pronounced increase in fluorescence intensity of HA and FA in SMP, DOM and HA in EPS were observed with increasing antibiotic stress, and the fluorescence intensity in R1 was significantly lower than that in R2. These all indicated that SDZ led to more membrane pollutants (DOM, HA and FA) in both SMP and EPS, and bioelectric fields could alleviate this situation and thus mitigate membrane fouling.

3.3. Microbial community diversity analysis

3.3.1. Suspended sludge

The diversity of microorganisms at the phylum level was shown in Fig. 5a. The composition displayed that all samples were typically dominated by *p_Actinobacteria, p_Chloroflexi, p_Euryarchaeota* and *p_Proteobacteria*, which accounted for about 80% of the total abundance. Among them, *p_Actinobacteria, p_Proteobacteria* and *p_Chloroflexi* played critical roles in anaerobic hydrolytic acidification [11]. *P_Actinobacteria* excelled at converting particulate matter such as carbohydrates, proteins, and fats into solutes and could generate acetic and propionic acid from glucose [49]. In phase S1, *p_Actinobacteria* occupied high abundance in R1 and R2, ensuring organic matter hydrolysis. In phase S2, *p_Actinobacteria* presented an increasing trend of 2.0% in R1 while a decreasing trend of 3.5% in R2, which may be related to the decrease in organic matter removal in R2. In phase S3, it was observed that the abundance of *p_Actinobacteria* showed a significant increase (8.8% and 14.6% in R1 and R2, respectively), indicating the strong survivability and degradation ability of *p_Actinobacteria* in the presence of SDZ [50]. *P_Chloroflexi* can degrade complex organics and accelerate the degradation of propionic acid and butyric acid to acetic acid [51]. In

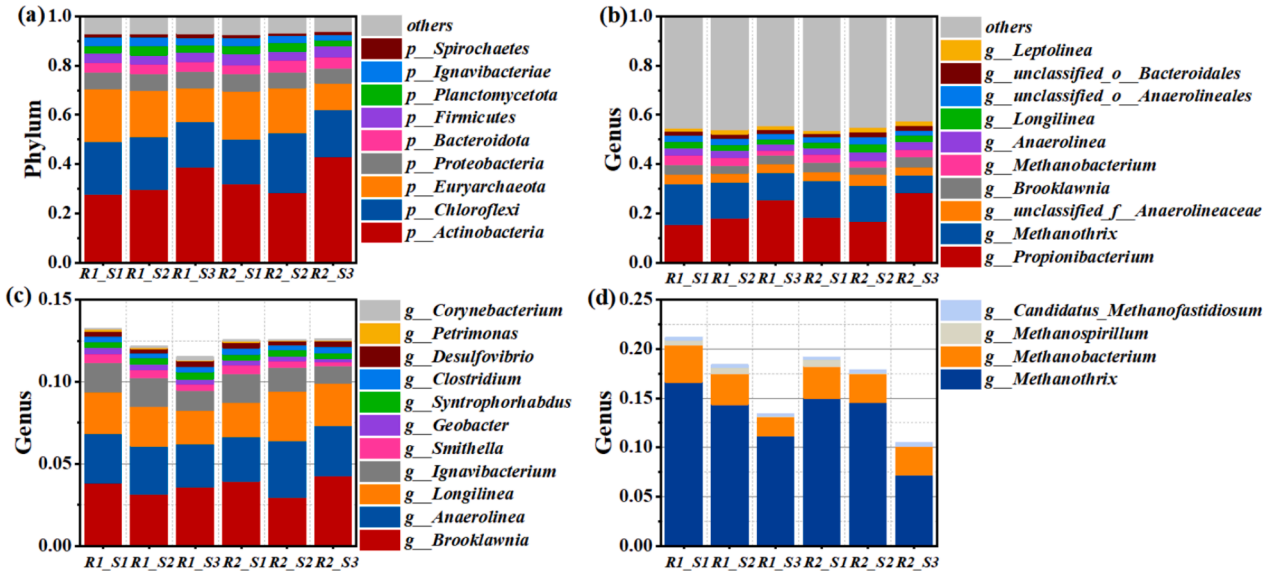

Fig. 5. Variation in microbial abundance at (a) phylum and (b) genus level, (c) variation in abundance of electroactive bacteria and (d) methanogen.

phase S1, the abundance of *p_Chloroflexi* in R1 and R2 was 21.2% and 18.3%, respectively, guaranteeing high organic matter removal in R1 and R2. Compared to R2, the higher abundance of *p_Chloroflexi* in R1 promoted more acetic acid formation, producing more methane. In addition, *p_Chloroflexi* was reported to have the ability to degrade SMP and EPS [52], so the increase in SMP and EPS concentrations due to antibiotic stress in phase S2 resulted in a significant increase in the abundance of *p_Chloroflexi* in R1 and R2. In phase S3, although more SMP and EPS were produced due to high antibiotic stress, it was possible that excessive antibiotics also seriously jeopardized the survival of *p_Chloroflexi*, which in turn led to a significant decrease in the abundance of *p_Chloroflexi* (2.7% and 5.2% in R1 and R1, respectively). Notably, *p_Euryarchaeota*, which contained various methanogenic genera, maintained a consistent trend in R1 and R2, gradually decreasing with increasing SDZ concentration, demonstrating the enhanced microbial growth inhibition as rising SDZ concentration. Its abundance in R1 was higher than in R2 in all phases, especially in phase S3, which was consistent with the observed methanogenic performance, suggesting the promotion of methanogenesis in R1 by the bioelectric field.

Analysis at the genus level showed that the dominant genera were *g_Propionibacterium*, *g_Methanothrix*, *g_unclassified_f_Anaerolineaceae*, *g_Brooklawnia* and *g_Methanobacterium* (Fig. 5b). Both *g_Propionibacterium* and *g_Brooklawnia* belonged to *p_Actinobacteria*, and most strains of *g_Propionibacterium* and *g_Brooklawnia* utilized glucose and produced propionic acid and acetic acid as fermentation end–products [53,54]. Their high abundance (20.4%–29.0% in R1 and 19.8%–32.5% in R2) throughout the operation ensured the degradation of glucose and the production of acetic acid and propionic acid, facilitating the anaerobic digestion. Their abundance gradually increased with the addition of SDZ, reaching a maximum in phase S3 (29.0% in R1 and 32.5% in R2), accompanied by a minimum abundance of methanogens (13.69% in R1 and 10.09% in R2), which caused the accumulation of acetic and propionic acids. In R1 and R2, *g_Methanothrix* (formally *g_Methanosaeta*), as a traditional acetoclastic methanogen, was the dominant methanogen due to its highest abundance in the whole operation period, followed by the hydrogenotrophic methanogen *g_Methanobacterium* (Fig. 5d). In phase S1, the abundance of methanogens in R1 and R2 was 21.2% and 19.2%, respectively. Therefore, the higher abundance of methanogens in R1 promoted the methanogenic performance. With the addition of SDZ, the abundance of methanogens exhibited a general decreasing trend in both R1 and R2, dropping to 13.4% in R1 and 10.5% in R2 in phase S3, which explained the decrease in methanogenic performance. Notably, methanogens in R1 were consistently higher than those in R2 throughout the experimental period, suggesting that the bioelectric field environment promoted the reproduction of methanogens even under severe antibiotic stress. In addition, *g_unclassified_f_Anaerolineaceae* was reported to be propionate–consuming bacteria [55]. The abundance was 4.0% in R1 and 3.5% in R2 in phase S1. The higher abundance in R1 suggested that the bioelectric field enriched *g_unclassified_f_Anaerolineaceae* to reduce the accumulation of propionic acid. After the SDZ addition, its abundance continuously reduced to 3.4% in R1 and 3.4% in R2. However, there was no further propionate accumulation, possibly due to the high proliferation of *g_Propionibacterium* (another propionate–consuming bacterium).

As can be seen from the variation of electroactive bacteria (Fig. 5c), *g_Brooklawnia*, *g_Anaerolinea*, *g_Longilinea*, and *g_Ignavibacterium* were the dominant electroactive bacteria. *G_Brooklawnia* can promote methanogenesis through direct interspecific electron transfer with *g_Methanosaeta* [54]. Both *g_Anaerolinea* and *g_Longilinea* belong to *c_Anaerolineae*, which can transfer electrons extracellularly to *g_Methanosaeta* during the oxidation of organic matter [56,57]. The electroactive bacteria *g_Ignavibacterium* was a key electroactive species involved in electron transfer of anaerobic degradation, capable of organic fermentation and H_2 oxidation [58]. In phase S1, the abundance of electroactive bacteria in R1 was significantly higher than that in R2, which indicated that the bioelectric field enriched more electroactive bacteria, which promoted methanogenic performance through electron transfer with methanogens. With the increase of SDZ concentration, the abundance of electroactive bacteria in R1 gradually decreased, consistent with the change of *g_Methanosaeta*, which ultimately caused a reduction in methane production. In contrast, the abundance of electroactive bacteria remained stable in R2. Analysis of Fig. 5c suggested that this was mainly due to the increased abundance of *g_Anaerolinea* and *g_Longilinea*. It had been reported that *c_Anaerolineae* (containing *g_Anaerolinea* and *g_Longilinea*) was a known EPS–fermenting bacterium [59]. Therefore, the increased abundance of *g_Anaerolinea* and *g_Longilinea* in R2 may be related to the secretion of more EPS under antibiotic stress.

3.3.2. *Sludge attached to the membrane*

As can be seen from the analysis of the microbial community attached to the membrane shown in Fig. 6, *p_Spirochaetota,*

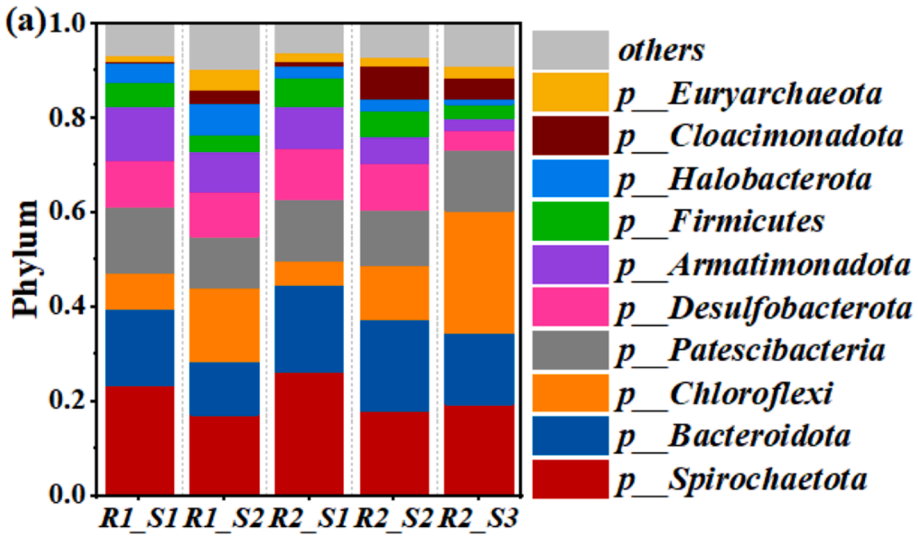

Fig. 6. Variation in abundance at the phylum level (R2_S3 was sampled at 105d, the biomass on the membrane is not enough for microbial analysis in R1 in phase_S3).

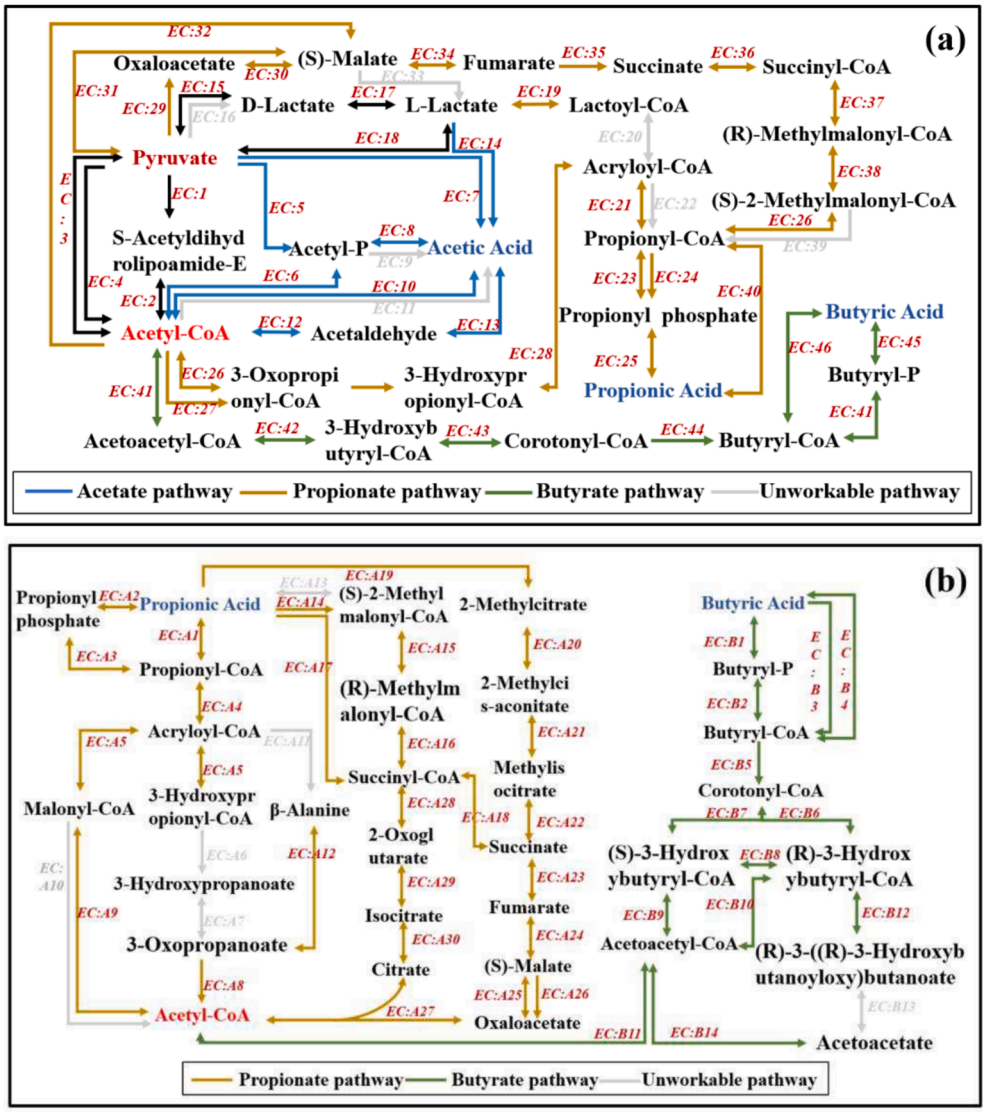

Fig. 7. (a) VFAs production pathway and (b) VFAs metabolism pathway.

p_Bacteroidota, p_Chloroflexi and *p_Patescibacteria* were the dominant species, accounting for 60%–70% throughout the experiment. Among them, *p_Spirochaetota* and *p_Patescibacteria* were commonly found in sewer biofilms and hypothesized to play a role in biofilm formation [60,61]. Therefore, compared to R2, the lower abundance of *p_Spirochaetota* and *p_Patescibacteria* in R1 was conducive to delaying the membrane fouling. Additionally, *p_Bacteroidota* is the key bacterium involved in membrane fouling, with relatively high abundances in both R1 (11.4%–16.2%) and R2 (15.1%–19.3%) [62]. According to Gao et al.'s research, *p_Bacteroidota* attaching to the membrane surface contributes to membrane fouling due to the release of proteinaceous EPS [63]. Thus, the significantly lower relative abundance of *p_Bacteroidota* in R1 was beneficial for lowering the formation of membrane fouling. Relatively high abundance of *p_Chloroflexi* was observed in both R1 (7.8%–15.4%) and R2 (5.3%–11.7%) in phases S1 and S2. As is well known, *p_Chloroflexi* can degrade and utilize proteins and polysaccharides [64]. Thus, a higher abundance of *p_Chloroflexi* in R1 can reduce the accumulation of pollutants (EPS and SMP) on the membrane surface. Moreover, *p_Firmicutes*, commonly detected in fouling layers, can accelerate biofouling in AnMBR [41]. The abundance of *p_Firmicutes* in R1 was lower than that in R2, which also indicated the slower development of membrane fouling in R1.

3.4. Genetic analysis

3.4.1. Pathways for VFAs

The acetate production pathway involved the enzymes EC:1–18, where the relative abundance of enzymes EC:9, 11 and 16 were 0 (Fig. 7a and Fig. S3a). In phase S1, the abundance of 11 enzymes in R1 was higher than in R2, and it was reasonable to assume that acetate–producing activity was significantly enhanced via the bioelectric field. Also, the methanogenic activity of R1 was superior to that of R2 during this phase (*detailed in section 3.4.2*), thus promoting the subsequent methanogenic process. In phases S2 and S3, the abundance of 7 enzymes increased in R1, and 11 and 8 enzymes increased in R2, respectively, and the total enzyme abundance increased with increasing antibiotic concentration in both R1 and R2. It was reasonable to suggest that antibiotics stress promoted acetate production [65].

Meanwhile, there was a marked decrease in the abundance of acetoclastic methanogenic enzymes in both R1 and R2 (*detailed in sections 3.4.2*), which inevitably led to an increase in acetate accumulation, which is precisely what happened. During this period, the abundance of acetoclastic methanogenic enzymes was much higher in R1 than in R2, and the abundance of acetate production enzymes was lower than in R2 (0.43%–0.61% lower than R2). All of these could be inferred that the bioelectric field alleviated the problems of acidification and low methanogenesis in the AnMBR system facing antibiotic stress.

Propionate production included three pathways: the Acetyl–CoA pathway (EC:1–4 and 21–28), the Lactate pathway (EC:16–25, where EC:20 was 0), and the Oxaloacetate pathway (EC:29–40 and 23–25). Propionate metabolism to acetate, butyrate production and butyrate metabolism to acetate pathways involved enzymes EC: A1–A30 (where EC: A6–7, 10–11 and 13 were 0), EC:1–4 and 41–46, and EC: B1–B14 (where EC: B13 was 0), respectively (Fig. 7 and S3). In phase S1, more than half of the enzyme abundances in propionate and butyrate production (and metabolism) and total enzyme abundances were higher in R1 than in R2, inferring that R1 exhibited more robust production and metabolism of propionate and butyrate due to the bioelectric field. In phase S2, more than half of the enzyme abundances in propionate production were down–regulated in R1 (12/21) and up–regulated in R2 (13/21). More than half of the enzymes in propionate metabolism were up–regulated in both R1 and R2 (14/25 and 20/25). Such variations could be reasonably inferred that exposure to SDZ facilitated the conversion of propionate to acetate. More than half of the enzymes in butyrate production were up–regulated, and more than half of the enzymes in butyrate metabolism were down–regulated in R1 and R2, inevitably leading to butyrate accumulation. All those showed that the effects of SDZ on different VFAs were inconsistent. In phase S3, more than half of the enzymes in propionate (and butyrate) production and metabolism and total enzyme abundances were up–regulated in both R1 and R2, and the abundance of propionate (and butyrate) metabolizing enzymes increased more than producing enzymes. All these can be inferred from the fact that the conversion of propionate (and butyrate) to acetate was further facilitated under the high antibiotic stress, leading to acetate accumulation. Notably, the increment of enzyme abundance in R1 was consistently smaller than in R2 during this phase (4.31% (0.06%) and 8.06% (2.04%) in propionate (butyrate) production of R1 and R2, 6.44% (6.84%) and 9.32% (16.11%) in propionate (butyrate) metabolism of R1 and R2), suggesting that the bioelectric field enhanced the system's ability to resist antibiotic stress.

The contribution of different species to the enzymes was analyzed to investigate which species were the primary sources of these enzymes (Fig. S4). Analysis of microbial contributions showed that *g_Propionibacterium* contributed significantly to acetate and propionate production, indicating that both acetate and propionate were metabolites of *g_Propionibacterium*. In addition, *g_Brooklawnia* and *g_unclassified_f_Anaerolineales* also contributed to acetate production, and the total abundance of these bacteria showed an increase with antibiotic dosing, which ultimately contributed to the gradual accumulation of acetate. In addition to *g_Propionibacterium* contributing to propionate production, *g_Brooklawnia* and *g_Anaerolinea* also contributed to propionate production. The total abundance of these bacteria also showed an increase with antibiotic dosing, which contributed significantly to propionate accumulation. Regarding propionate metabolism, *g_Propionibacterium* also contributed significantly, suggesting that the final fermentation product of *g_Propionibacterium* may be acetate. With the addition of antibiotics, the gradually increasing abundance of *g_Propionibacterium* promoted the conversion of propionate to acetate. In addition, *g_Ignavibacterium*, *g_Brooklawnia*, and *g_Anaerolinea* also contributed to propionate metabolism. Butyrate production was dominated by *g_Propionibacterium*, *g_Anaerolinea*, and *g_Ignavibacterium*; *g_Propionibacterium*, *g_Syntrophomonas*, and *g_Smithella* dominated butyrate metabolism. *G_Propionibacterium* played a role in butyrate production and metabolism, suggesting that acetate was the end product. It was noteworthy that in phase S2, as the abundance of functional bacteria with butyrate metabolism increased, the abundance of butyrate metabolizing enzymes decreased, which presumably may be related to the gene expression of the functional bacteria, which needs to be further investigated.

3.4.2. Pathways for methane

The intrinsic methanogenic mechanisms under the bioelectric field and SDZ exposure were explored by analyzing the methanogenic pathway and related enzyme genes. As shown in Fig. 8, methanogenesis consists of two pathways: the acetoclastic methanogenesis pathway (EC:1–4 and 13–14) and the hydrogenotrophic methanogenesis pathway (EC:5–14). From the enzyme abundances (Fig. S5), the acetoclastic methanogenesis pathway was the main pathway. Acetyl–CoA was vital in the acetoclastic methanogenesis pathway. The production of Acetyl–CoA was divided into two ways: one is the production of Acetyl–P by Acetic acid through EC:1, and then Acetyl–CoA through EC:2. The other is the production of Acetyl–CoA by Acetic acid through EC:3. Apparently, the second one from the enzymes abundance and shorter reaction chain may be the main pathway. In phase S1, the abundance of 13 enzymes was significantly higher in R1 than in R2, especially the critical enzyme EC:3 and universal enzymes EC:13–14, corresponding to the high methane production in R1. It was inferred that the bioelectric field significantly increased the abundance of methanogenic enzymes, promoting higher methane production and avoiding system acidification. In phases S2 and S3, the enzyme abundances in the methanogenic pathway showed a gradual decrease in both R1 and R2, which can be inferred that the inhibition of methanogenic performance was also progressively

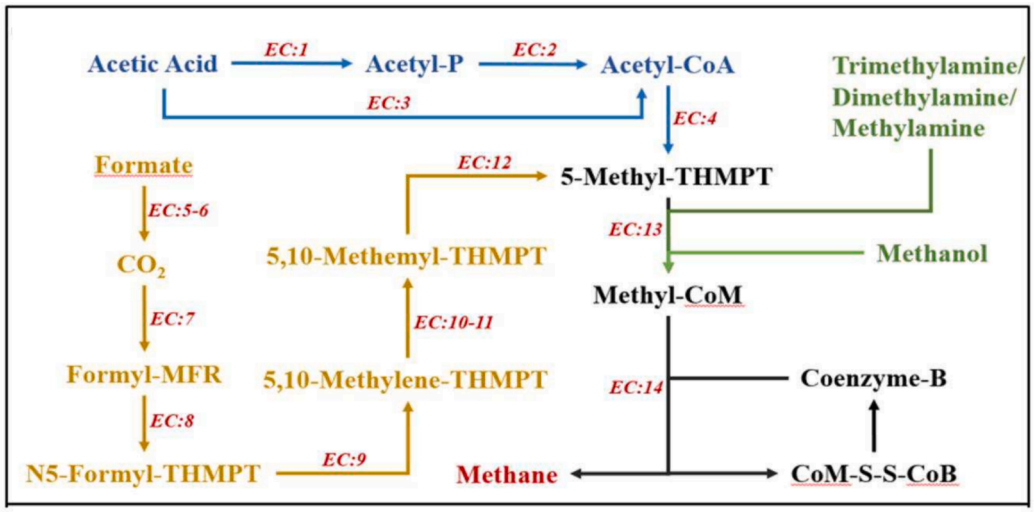

Fig. 8. Pathways for methanogenesis.

severe with increasing antibiotic concentration. Compared to R2, the abundance of the relevant methanogenic enzymes in R1 was still higher, suggesting that the bioelectric field could enhance the ability of methanogens to counteract antibiotic stress. Analysis of microbial contributions indicated that *g_Methanothrix* and *g_Methanobacterium* species play a significant role in methanogenesis, and variations in their abundances were also consistent with changes in the abundance of methanogenic enzymes.

3.4.3. Antibiotic resistance genes

Variations in gene expression quantities (FPKM) of antibiotic resistance genes (ARGs) were further analyzed (Fig. 9a). All sul1–4 were dihydropteroate synthase genes and mobile sulfonamide resistance genes shown to confer resistance when expressed in microorganisms. It can be seen that ARG changes in R1 and R2 were similar, with the abundance increasing in phase S2 while decreasing in phase S3. This indicated that the low–concentration antibiotic environment may promote the reproduction of resistant microorganisms and the enrichment of ARGs through selection. In contrast, the high–concentration antibiotic environment may cause great stress to the microbial community, leading to the death of resistant microorganisms and decreasing the abundance of ARGs to some extent. Moreover, the ARGs in R1 were consistently higher than in R2 throughout the experimental period, consistent with the studies of Zhang and Yuan et al., indicating that the relative abundance of ARGs was increased by bioelectric field stimulation [27,66]. According to previous research, this phenomenon was related to the fact that the host microorganisms of ARGs could survive by respiring anode electrodes and electron shuttles released by exoelectrogens, thereby promoting the enrichment of ARGs [66].

The species contributions to the ARGs were analyzed to explore the sources (Fig. 9b). According to the analysis, the enrichment of sul4 was mainly associated with *g_Propionibacterium*, *g_Longilinea* and *g_Brooklawnia*, sul3 was mainly associated with *g_Methanothrix*, and sul1 was associated with *g_Escherichia* and *g_Treponema* and *g_Methanothrix*. All of this suggested that these bacteria may be potential hosts for ARGs, and the enrichment of potential ARG hosts in R1 and R2 may be the reason for the difference in ARG abundance. Furthermore, it was worth noting that *g_Brooklawnia* and *g_Longilinea* are exoelectrogens, whereas *g_Escherichia* and *g_Methanothrix* could use electrons released by exoelectrogens for metabolism [15,66]. Although not all of these species

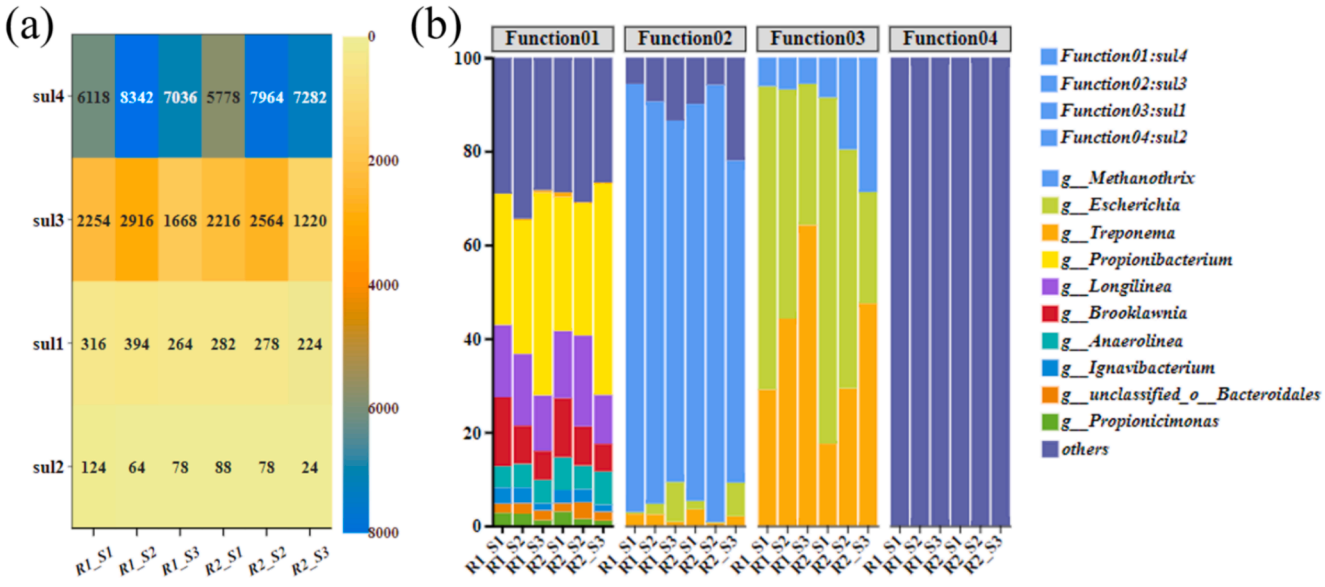

Fig. 9. (a) Variations in gene expression quantities (FPKM) of ARGs and (b) species contribution to the ARGs.

were more abundant in R1 than in R2, the bioelectric field may have promoted the activity of these microorganisms, which in turn increased the expression of ARGs in R1.

4. Conclusion

This study focused on the operational performance of a bioelectric field-enhanced anaerobic membrane bioreactor (AnMBR) system dealing with swine wastewater (SW) under varying sulfadiazine (SDZ) concentration stresses. The key findings are as follows:

(1) Impact on COD removal and methane production

SDZ inhibited COD removal and methane production, causing a significant build-up of VFAs. The inhibitory effect was more intense when SDZ concentrations increased. However, the bioelectric field effectively counteracted these negative impacts.

(2) Effect on SMP/EPS production and membrane fouling

SDZ promoted the production of SMP and EPS in the AnMBR, which aggravated membrane fouling. Fortunately, the bioelectric field significantly decreased the levels of SMP and EPS, thus prolonging the membrane fouling cycle even when SDZ was present.

(3) Microbiological analysis results

Microbiological analysis indicated that SDZ suppressed the abundance of *g_Methanosaeta*, leading to VFA accumulation and reduced methane production. The bioelectric field, on the other hand, significantly alleviated this inhibition. The bioelectric field also enriched *p_Chloroflexi*, which helped mitigate membrane fouling pollutants. It also alleviated the formation of membrane fouling by reducing the presence of *p_Bacteroidota* and *p_Firmicutes* on membrane surfaces.

(4) Genetic analysis insights

Genetic analysis demonstrated that the bioelectric field alleviated SDZ-induced stress by stabilizing methanogenic enzyme levels and minimizing the overproduction of acetate-synthesizing enzymes.

(5) Overall implications and future research directions

This work presented an effective strategy for enhancing AnMBR systems in treating antibiotic-laden wastewater and provided a theoretical basis for practical applications. However, further research is necessary to explore the challenges associated with scaling up and to address the co-pollution from multiple antibiotics.

CRediT authorship contribution statement

Haojie Huang: Writing – original draft, Methodology, Investigation, Formal analysis. **Yutong Sun:** Methodology, Investigation. **Qing Du:** Writing – review & editing, Funding acquisition, Formal analysis, Data curation. **Fu Gao:** Resources, Formal analysis, Data curation. **Zi Song:** Writing – review & editing, Investigation. **Zhiwen Wang:** Writing – review & editing, Investigation. **Suyun Chang:** Resources, Formal analysis, Data curation. **Xinbo Zhang:** Writing – review & editing, Supervision, Project administration, Methodology, Funding acquisition. **Wenshan Guo:** Writing – review & editing, Investigation. **Huu Hao Ngo:** Writing – review & editing, Supervision, Investigation, Conceptualization.

Declaration of competing interest

The authors declare that they have no known competing financial interests or personal relationships that could have appeared to influence the work reported in this paper.

Acknowledgements

This research was supported by the National Natural Science Foundation of China (No.52400054) and Tianjin Municipal Science and Technology Bureau of China (No.20JCZDJC00380 and 18PTZWHZ00140).

Appendix A. Supplementary data

Supplementary data to this article can be found online at https://doi.org/10.1016/j.cej.2025.160225.

Data availability

Data will be made available on request.

References

[1] M. Kratzer, A. Haq, P. Parameswaran, B. Sturm, V. Khanna, Optimization based process modeling of an anaerobic membrane bioreactor system: Application to swine wastewater, Chem. Eng. J. 503 (2025) 158165, https://doi.org/10.1016/j.cej.2024.158165.

[2] Y. Lauzurique, S. Segura, S. Guerra, A. Carvajal, C. Huiliñir, I. Poblete-Castro, Enhancing methane production using various forms of steel shavings and their effect on microbial consortia during anaerobic digestion of swine wastewater, J. Environ. Chem. Eng. 12 (5) (2024) 113764, https://doi.org/10.1016/j.jece.2024.113764.

[3] L. Deng, D. Zheng, J. Zhang, H. Yang, L. Wang, W. Wang, T. He, Y. Zhang, Treatment and utilization of swine wastewater – A review on technologies in full-scale application, Sci. Total Environ. 880 (2023) 163223, https://doi.org/10.1016/j.scitotenv.2023.163223.

[4] W. Chetawan, S. Krishnan, K. Saritpongteeraka, A. Palamanit, D. Gabriel, S. Chaiprapat, Elucidating the role of sub-thermophilic temperature and pre-hydrolyzation for effective upgrading scheme of old swine manure digesters, Bioresour. Technol. 408 (2024) 131199, https://doi.org/10.1016/j.biortech.2024.131199.

[5] M. Guimarães de Oliveira, J.M. Marques Mourão, F.S. Souza Silva, A. Bezerra dos Santos, E. Lopes Pereira, Effect of microaerophilic treatment on swine wastewater (SWW) treatment: Engineering and microbiological aspects, Journal of Environmental Management 299 (2021) 113598, https://doi.org/10.1016/j.jenvman.2021.113598.

[6] G. Wang, G. Liu, G. Yao, P. Fu, C. Sun, Y. Li, Q. Li, Y.-Y. Li, R. Chen, Biochar-assisted anaerobic membrane bioreactor towards high-efficient energy recovery from swine wastewater: Performances and the potential mechanisms, Bioresour. Technol. 369 (2023) 128480, https://doi.org/10.1016/j.biortech.2022.128480.

[7] W. Liu, X. Song, X. Ding, R. Xia, X. Lin, G. Li, L.D. Nghiem, W. Luo, Antibiotic removal from swine farming wastewater by anaerobic membrane bioreactor: Role of hydraulic retention time, J. Membr. Sci. 677 (2023) 121629, https://doi.org/10.1016/j.memsci.2023.121629.

[8] J. Tang, Y. Pu, T. Zeng, Y. Hu, J. Huang, S. Pan, X.C. Wang, Y. Li, A.-E.-F. Abomohra, Enhanced methane production coupled with livestock wastewater treatment using anaerobic membrane bioreactor: Performance and membrane filtration properties, Bioresour. Technol. 345 (2022) 126470, https://doi.org/10.1016/j.biortech.2021.126470.

[9] A.S. Oberoi, K.C. Surendra, D. Wu, H. Lu, J.W.C. Wong, S. Kumar Khanal, Anaerobic membrane bioreactors for pharmaceutical-laden wastewater treatment: A critical review, Bioresource Technology 361 (2022) 127667, https://doi.org/10.1016/j.biortech.2022.127667.

[10] J. Ji, A. Kakade, Z. Yu, A. Khan, P. Liu, X. Li, Anaerobic membrane bioreactors for treatment of emerging contaminants: A review, J. Environ. Manage. 270 (2020) 110913, https://doi.org/10.1016/j.jenvman.2020.110913.

[11] H.H. Xinbo Zhang, Qing Du, Fu Gao, Zhiwen Wang, Guangxue Wu, Wenshan Guo, Huu Hao Ngo, Performance of a recirculated biogas-sparging anaerobic membrane bioreactor system for treating synthetic swine wastewater containing sulfadiazine antibiotic, Chemical Engineering Journal 476 (2024) 146735. https://doi.org/10.1016/j.cej.2023.146735.

[12] L. Zang, X.-L. Yang, H. Xu, Y.-G. Xia, H.-L. Song, A novel integrated microbial fuel cell-membrane bioreactor (MFC-MBR) for controlling the spread of antibiotic and antibiotic resistance genes while simultaneously alleviating membrane fouling, Chem. Eng. J. 487 (2024) 150578, https://doi.org/10.1016/j.cej.2024.150578.

[13] X. Yin, X. Li, Z. Hua, Y. Ren, The growth process of the cake layer and membrane fouling alleviation mechanism in a MBR assisted with the self-generated electric field, Water Res. 171 (2020) 115452, https://doi.org/10.1016/j.watres.2019.115452.

[14] Y. Liu, X. Cao, J. Zhang, Z. Fang, H. Zhang, X. Gao, X. Li, The use of a self-generated current in a coupled MFC-AnMBR system to alleviate membrane fouling, Chem. Eng. J. 442 (2022) 136090, https://doi.org/10.1016/j.cej.2022.136090.

[15] H. Huang, X. Zhang, Q. Du, F. Gao, Z. Wang, G. Wu, W. Guo, H. Hao Ngo, Assessing the Long-Term performance of an integrated microbial fuel Cell-Anaerobic membrane bioreactor for swine wastewater treatment, Chemical Engineering Journal 493 (2024) 152772, https://doi.org/10.1016/j.cej.2024.152772.
[16] A. Raza Altaf, S. Raza, Y. Wang, F. Liu, Y.G. Adewuyi, P. Liu, Electrocatalytic arsenic removal: Unveiling selective capturing and conversion with a redox-active silica-lignosulfonate hybrid framework, Chemical Engineering Journal 499 (2024), https://doi.org/10.1016/j.cej.2024.156384.
[17] A.R. Khan, W. Wang, A.R. Altaf, S. Shaukat, H.-J. Zhang, A.U. Rehman, Z. Jun, L. Peng, Facial Synthesis, Stability, and Interaction of Ti3C2Tx@PC Composites for High-Performance Biocathode Microbial Electrosynthesis Systems, ACS Omega 8 (33) (2023) 29949–29958, https://doi.org/10.1021/acsomega.2c08163.
[18] B. Hou, X. Liu, R. Zhang, Y. Li, P. Liu, J. Lu, Investigation and evaluation of membrane fouling in a microbial fuel cell-membrane bioreactor systems (MFC-MBR), Sci. Total Environ. 814 (2022) 152569, https://doi.org/10.1016/j.scitotenv.2021.152569.
[19] M.H. McCrady, Standardmethods for the examination of water and waste-water, American Journal of Public Health and the Nations Health 56(4) (1966) 684, https://doi.org/10.2105/AJPH.56.4.684-a.
[20] X. Lu, G. Zhen, Y. Liu, T. Hojo, A.L. Estrada, Y.-Y. Li, Long-term effect of the antibiotic cefalexin on methane production during waste activated sludge anaerobic digestion, Bioresour. Technol. 169 (2014) 644–651, https://doi.org/10.1016/j.biortech.2014.07.056.
[21] Q. Du, Q. Mu, G. Wu, Metagenomic and bioanalytical insights into quorum sensing of methanogens in anaerobic digestion systems with or without the addition of conductive filter, Sci. Total Environ. 763 (2021) 144509, https://doi.org/10.1016/j.scitotenv.2020.144509.
[22] W. Yan, Y. Guo, Y. Xiao, S. Wang, R. Ding, J. Jiang, H. Gang, H. Wang, J. Yang, F. Zhao, The changes of bacterial communities and antibiotic resistance genes in microbial fuel cells during long-term oxytetracycline processing, Water Res. 142 (2018) 105–114, https://doi.org/10.1016/j.watres.2018.05.047.
[23] S.P. Tan, H.F. Kong, M.J.K. Bashir, P.K. Lo, C.-D. Ho, C.A. Ng, Treatment of palm oil mill effluent using combination system of microbial fuel cell and anaerobic membrane bioreactor, Bioresour. Technol. 245 (2017) 916–924, https://doi.org/10.1016/j.biortech.2017.08.202.
[24] F. Meng, L. Feng, H. Yin, K. Chen, G. Hu, G. Yang, J. Zhou, Assessment of nutrient removal and microbial population dynamics in a non-aerated vertical baffled flow constructed wetland for contaminated water treatment with composite biochar addition, J. Environ. Manage. 246 (2019) 355–361, https://doi.org/10.1016/j.jenvman.2019.06.011.
[25] J. Wilkinson, P.S. Hooda, J. Barker, S. Barton, J. Swinden, Occurrence, fate and transformation of emerging contaminants in water: An overarching review of the field, Environ. Pollut. 231 (2017) 954–970, https://doi.org/10.1016/j.envpol.2017.08.032.
[26] Z. Wang, J. Gao, Y. Zhao, Y. Cui, Y. Zhang, H. Dai, D. Li, Discrepant responses of polyvinyl chloride microplastics biofilms and activated sludge under sulfadiazine stress in an anaerobic/anoxic/oxic system, Chem. Eng. J. 446 (2022) 137055, https://doi.org/10.1016/j.cej.2022.137055.
[27] S. Zhang, H.-L. Song, X. Cao, H. Li, J. Guo, X.-L. Yang, R.P. Singh, S. Liu, Inhibition of methanogens decreased sulfadiazine removal and increased antibiotic resistance gene development in microbial fuel cells, Bioresour. Technol. 281 (2019) 188–194, https://doi.org/10.1016/j.biortech.2019.02.089.
[28] X. Zhang, Z. Song, H. Hao Ngo, W. Guo, Z. Zhang, Y. Liu, D. Zhang, Z. Long, Impacts of typical pharmaceuticals and personal care products on the performance and microbial community of a sponge-based moving bed biofilm reactor, Bioresource Technology 295 (2020) 122298, https://doi.org/10.1016/j.biortech.2019.122298.
[29] W. Xu, B. Yang, H. Wang, L. Zhang, J. Dong, C. Liu, Simultaneous removal of antibiotics and nitrogen by microbial fuel cell-constructed wetlands: Microbial response and carbon–nitrogen metabolism pathways, Sci. Total Environ. 893 (2023) 164855, https://doi.org/10.1016/j.scitotenv.2023.164855.
[30] D. Cheng, H.H. Ngo, W. Guo, D. Lee, D.L. Nghiem, J. Zhang, S. Liang, S. Varjani, J. Wang, Performance of microbial fuel cell for treating swine wastewater containing sulfonamide antibiotics, Bioresour. Technol. 311 (2020) 123588, https://doi.org/10.1016/j.biortech.2020.123588.
[31] D. Hu, L. Liu, W. Liu, L. Yu, J. Dong, F. Han, H. Wang, Z. Chen, H. Ge, B. Jiang, X. Wang, Y. Cui, W. Zhang, Y. Zhang, S. Liu, L. Zhao, Improvement of sludge characteristics and mitigation of membrane fouling in the treatment of pesticide wastewater by electrochemical anaerobic membrane bioreactor, Water Res. 213 (2022) 118153, https://doi.org/10.1016/j.watres.2022.118153.
[32] D.L. Cheng, H.H. Ngo, W.S. Guo, S.W. Chang, D.D. Nguyen, S.M. Kumar, B. Du, Q. Wei, D. Wei, Problematic effects of antibiotics on anaerobic treatment of swine wastewater, Bioresour. Technol. 263 (2018) 642–653, https://doi.org/10.1016/j.biortech.2018.05.010.
[33] S. Aydin, Z. Cetecioglu, O. Arikan, B. Ince, E.G. Ozbayram, O. Ince, Inhibitory effects of antibiotic combinations on syntrophic bacteria, homoacetogens and methanogens, Chemosphere 120 (2015) 515–520, https://doi.org/10.1016/j.chemosphere.2014.09.045.
[34] W. Xu, M. Luo, X. Lu, Z. Ye, T. Jeong, Simultaneous Removal of Nitrate and Tetracycline by an Up-Flow Immobilized Biofilter, Water (2022).
[35] H. Cheng, Y. Li, Y. Hu, G. Guo, M. Cong, B. Xiao, Y.-Y. Li, Bioenergy recovery from methanogenic co-digestion of food waste and sewage sludge by a high-solid anaerobic membrane bioreactor (AnMBR): mass balance and energy potential, Bioresour. Technol. 326 (2021) 124754, https://doi.org/10.1016/j.biortech.2021.124754.
[36] Z. Jiang, Z. Xia, S. Liu, Q. Wei, H. Fan, L. Qi, G. Liu, H. Wang, The effect of fine grits and fine debris concentrations on the MLVSS/MLSS ratio of an activated sludge system, J. Environ. Sci. 147 (2023) 607–616, https://doi.org/10.1016/j.jes.2023.10.032.
[37] D. Cheng, H.H. Ngo, W. Guo, S.W. Chang, D.D. Nguyen, Q.A. Nguyen, J. Zhang, S. Liang, Improving sulfonamide antibiotics removal from swine wastewater by supplying a new pomelo peel derived biochar in an anaerobic membrane bioreactor, Bioresour. Technol. 319 (2021) 124160, https://doi.org/10.1016/j.biortech.2020.124160.
[38] D. Cheng, H.H. Ngo, W. Guo, S.W. Chang, D.D. Nguyen, Y. Liu, Y. Liu, L. Deng, Z. Chen, Evaluation of a continuous flow microbial fuel cell for treating synthetic swine wastewater containing antibiotics, Sci. Total Environ. 756 (2021) 144133, https://doi.org/10.1016/j.scitotenv.2020.144133.
[39] A. Aslam, S.J. Khan, H.M.A. Shahzad, Anaerobic membrane bioreactors (AnMBRs) for municipal wastewater treatment- potential benefits, constraints, and future perspectives: An updated review, Sci. Total Environ. 802 (2022) 149612, https://doi.org/10.1016/j.scitotenv.2021.149612.
[40] Z. Lei, J. Wang, L. Leng, S. Yang, M. Dzakpasu, Q. Li, Y.-Y. Li, X.C. Wang, R. Chen, New insight into the membrane fouling of anaerobic membrane bioreactors treating sewage: Physicochemical and biological characterization of cake and gel layers, J. Membr. Sci. 632 (2021) 119383, https://doi.org/10.1016/j.memsci.2021.119383.
[41] D. Cheng, H.H. Ngo, W. Guo, Y. Liu, S.W. Chang, D.D. Nguyen, L.D. Nghiem, J. Zhou, B. Ni, Anaerobic membrane bioreactors for antibiotic wastewater treatment: Performance and membrane fouling issues, Bioresour. Technol. 267 (2018) 714–724, https://doi.org/10.1016/j.biortech.2018.07.133.
[42] M. Yao, B. Ladewig, K. Zhang, Identification of the change of soluble microbial products on membrane fouling in membrane bioreactor (MBR), Desalination 278 (1–3) (2011) 126–131, https://doi.org/10.1016/j.desal.2011.05.012.
[43] X. Xiang, J. Bai, W. Gu, S. Peng, K. Shih, Mechanism and application of modified bioelectrochemical system anodes made of carbon nanomaterial for the removal of heavy metals from soil, Chemosphere 345 (2023) 140431, https://doi.org/10.1016/j.chemosphere.2023.140431.
[44] S.F. Aquino, D.C. Stuckey, Soluble microbial products formation in anaerobic chemostats in the presence of toxic compounds, Water Res. 38 (2) (2004) 255–266, https://doi.org/10.1016/j.watres.2003.09.031.
[45] Y. Zhu, Y. Wang, S. Zhou, X. Jiang, X. Ma, C. Liu, Robust performance of a membrane bioreactor for removing antibiotic resistance genes exposed to antibiotics: Role of membrane foulants, Water Res. 130 (2018) 139–150, https://doi.org/10.1016/j.watres.2017.11.067.
[46] Y. Ding, Y. Tian, Z. Li, W. Zuo, J. Zhang, A comprehensive study into fouling properties of extracellular polymeric substance (EPS) extracted from bulk sludge and cake sludge in a mesophilic anaerobic membrane bioreactor, Bioresour. Technol. 192 (2015) 105–114, https://doi.org/10.1016/j.biortech.2015.05.067.
[47] H. Sun, H. Liu, J. Han, X. Zhang, F. Cheng, Y. Liu, Chemical cleaning-associated generation of dissolved organic matter and halogenated byproducts in ceramic MBR: Ozone versus hypochlorite, Water Res. 140 (2018) 243–250, https://doi.org/10.1016/j.watres.2018.04.050.
[48] Y. Liu, Q. Liu, J. Li, H.H. Ngo, W. Guo, J. Hu, M.-T. Gao, Q. Wang, Y. Hou, Effect of magnetic powder on membrane fouling mitigation and microbial community/composition in membrane bioreactors (MBRs) for municipal wastewater treatment, Bioresour. Technol. 249 (2018) 377–385, https://doi.org/10.1016/j.biortech.2017.10.027.
[49] J. De Vrieze, A.M. Saunders, Y. He, J. Fang, P.H. Nielsen, W. Verstraete, N. Boon, Ammonia and temperature determine potential clustering in the anaerobic digestion microbiome, Water Res 75 (2015) 312–323, https://doi.org/10.1016/j.watres.2015.02.025.
[50] C. Tian, R. Dai, M. Chen, X. Wang, W. Shi, J. Ma, Z. Wang, Biofouling suppresses effluent toxicity in an electrochemical filtration system for remediation of sulfanilic acid-contaminated water, Water Res. 219 (2022) 118545, https://doi.org/10.1016/j.watres.2022.118545.
[51] Q. Fan, Z. Shao, X. Guo, Q. Qu, Y. Yao, Z. Zhang, L. Qiu, Effects of Fe–N co-modified biochar on methanogenesis performance, microbial community, and metabolic pathway during anaerobic co-digestion of alternanthera philoxeroides and cow manure, J. Environ. Manage. 351 (2024) 120006, https://doi.org/10.1016/j.jenvman.2023.120006.
[52] C. Chen, M. Sun, J. Chang, Z. Liu, X. Zhu, K. Xiao, G. Song, H. Wang, G. Liu, X. Huang, Unravelling temperature-dependent fouling mechanism in a pilot-scale anaerobic membrane bioreactor via statistical modelling, J. Membr. Sci. 644 (2022) 120145, https://doi.org/10.1016/j.memsci.2021.120145.
[53] T. Ito, K. Yoshiguchi, H.D. Ariesyady, S. Okabe, Identification and quantification of key microbial trophic groups of methanogenic glucose degradation in an anaerobic digester sludge, Bioresour. Technol. 123 (2012) 599–607, https://doi.org/10.1016/j.biortech.2012.07.108.
[54] W. Wu, S.G. Arhin, H. Sun, Z. Li, Z. Yang, G. Liu, W. Wang, Facilitated CO biomethanation by exogenous materials via inducing specific methanogenic pathways, Chem. Eng. J. 460 (2023) 141736, https://doi.org/10.1016/j.cej.2023.141736.
[55] L. Xie, J. Zhu, J. Xie, J. Xu, R. He, W. Wang, Underlying the inhibition mechanisms of sulfate and lincomycin on long-term anaerobic digestion: Microbial response and antibiotic resistance genes distribution, Sci. Total Environ. 915 (2024) 169837, https://doi.org/10.1016/j.scitotenv.2023.169837.
[56] Y. Zheng, X. Quan, M. Zhuo, X. Zhang, Y. Quan, In-situ formation and self-immobilization of biogenic Fe oxides in anaerobic granular sludge for enhanced performance of acidogenesis and methanogenesis, Sci. Total Environ. 787 (2021) 147400, https://doi.org/10.1016/j.scitotenv.2021.147400.

[57] J. Xu, J. Xie, Y. Wang, L. Xu, Y. Zong, W. Pang, L. Xie, Effect of anthraquinone-2,6-disulfonate (AQDS) on anaerobic digestion under ammonia stress: Triggering mediated interspecies electron transfer (MIET), Sci. Total Environ. 828 (2022) 154158, https://doi.org/10.1016/j.scitotenv.2022.154158.

[58] M. Zheng, J. Shi, C. Xu, Y. Han, Z. Zhang, H. Han, Insights into electroactive biofilms for enhanced phenolic degradation of coal pyrolysis wastewater (CPW) by magnetic activated coke (MAC): Metagenomic analysis in attached biofilm and suspended sludge, J. Hazard. Mater. 395 (2020) 122688, https://doi.org/10.1016/j.jhazmat.2020.122688.

[59] Y. Zhao, B. Jiang, X. Tang, S. Liu, Metagenomic insights into functional traits variation and coupling effects on the anammox community during reactor start-up, Sci. Total Environ. 687 (2019) 50–60, https://doi.org/10.1016/j.scitotenv.2019.05.491.

[60] W. Pan, H. Ouyang, X. Tan, R. Deng, L. Gu, Q. He, Anaerobic dynamic membrane bioreactors for synthetic blackwater treatment under room temperature and mesophilic conditions, Bioresour. Technol. 355 (2022) 127295, https://doi.org/10.1016/j.biortech.2022.127295.

[61] A. Liu, W. Lin, R. Ming, W. Guan, X. Wang, N. Hu, Y. Ren, Stability of 28 typical prescription drugs in sewer systems and interaction with the biofilm bacterial community, J. Hazard. Mater. 436 (2022) 129142, https://doi.org/10.1016/j.jhazmat.2022.129142.

[62] J. Ma, Z. Wang, X. Zou, J. Feng, Z. Wu, Microbial communities in an anaerobic dynamic membrane bioreactor (AnDMBR) for municipal wastewater treatment: Comparison of bulk sludge and cake layer, Process Biochem. 48 (3) (2013) 510–516, https://doi.org/10.1016/j.procbio.2013.02.003.

[63] D.-W. Gao, T. Zhang, C.-Y.-Y. Tang, W.-M. Wu, C.-Y. Wong, Y.H. Lee, D.H. Yeh, C. S. Criddle, Membrane fouling in an anaerobic membrane bioreactor: Differences in relative abundance of bacterial species in the membrane foulant layer and in suspension, J. Membr. Sci. 364 (1–2) (2010) 331–338, https://doi.org/10.1016/j.memsci.2010.08.031.

[64] C. Juntawang, C. Rongsayamanont, E. Khan, Entrapped cells-based-anaerobic membrane bioreactor treating domestic wastewater: Performances, fouling, and bacterial community structure, Chemosphere 187 (2017) 147–155, https://doi.org/10.1016/j.chemosphere.2017.08.113.

[65] Y. Xiang, W. Xiong, R. Xu, Z. Yang, Y. Zhang, M. Jia, H. Peng, Metagenomic analysis reveals microbial metabolic potentials alterations under antibiotic stress during sludge anaerobic digestion, J. Environ. Chem. Eng. 11 (5) (2023) 110746, https://doi.org/10.1016/j.jece.2023.110746.

[66] H. Yuan, J.H. Miller, I.M. Abu-Reesh, A. Pruden, Z. He, Effects of electron acceptors on removal of antibiotic resistant Escherichia coli, resistance genes and class 1 integrons under anaerobic conditions, Sci. Total Environ. 569–570 (2016) 1587–1594, https://doi.org/10.1016/j.scitotenv.2016.07.002.